Proc. Natl. Acad. Sci. USA
Vol. 86, pp. 529–533, January 1989
Biophysics

Replacement of aspartic residues 85, 96, 115, or 212 affects the quantum yield and kinetics of proton release and uptake by bacteriorhodopsin

(site-specific mutagenesis/proton pump/differential conductivity/membrane protein/interfacial charge transfer)

TIM MARINETTI*, SRIRAM SUBRAMANIAM†, TATSUSHI MOGI†, THOMAS MARTI†, AND H. GOBIND KHORANA†

*Biophysics Laboratory, Rockefeller University, 1230 York Avenue, New York, NY 10021; and †Departments of Biology and Chemistry, Massachusetts Institute of Technology, 77 Massachusetts Avenue, Cambridge, MA 02139

Contributed by H. Gobind Khorana, October 24, 1988

ABSTRACT **Recently, a number of aspartic acid mutants of bacteriorhodopsin have been shown to be defective in steady-state proton transport. Here we report time-resolved measurements of light-induced proton release and uptake for these mutants. Proton transfers between the protein and the aqueous phase were directly monitored by measuring changes in the bulk conductivity of a micellar solution of bacteriorhodopsin. For the Asp-96 → Asn mutant, proton uptake was slowed by >1 order of magnitude with no observable effect on the release step. For Asp-85 → Asn, H^+ uptake occurred with normal kinetics, but the yield was significantly lower compared with either the Asp-96 → Asn mutant or wild type, especially at pH 6. Substitution of glutamate for Asp-85 or Asp-96 had smaller but detectable effects on the kinetics and quantum yield of proton movements. Both asparagine and glutamate substitutions of aspartates at positions 115 and 212 lowered the proton quantum yields. Of these, only the Asp-115 → Asn mutant showed an effect on the proton release step, and only the Asp-212 → Glu mutation decreased the proton uptake rate. These experiments imply an obligatory role for Asp-96 in H^+ uptake in the normal operation of the bacteriorhodopsin proton pump. The results also indicate that the amino acid substitutions affect the kinetics of either H^+ release or H^+ uptake, but not both. This implies that the two steps occur independently of each other after initiation of the photocycle.**

Bacteriorhodopsin (bR) is the sole polypeptide component of the purple membrane from *Halobacterium halobium* and functions as a light-driven proton pump (1, 2). Absorption of a photon triggers isomerization of the protein-linked retinal (3, 4) and initiates a photocycle, during which protons are released on the extracellular side and taken up on the cytoplasmic side of the molecule (5–7). Fourier transform infrared spectroscopic experiments have demonstrated protonation changes in carboxyl groups during the photocycle (8, 9), which were later shown to be specifically due to aspartate residues (10).

By using the techniques of site-specific mutagenesis, a variety of amino acid substitutions have been carried out in bR (11). Biochemical characterization of the mutant proteins has resulted in the identification of a small set of residues that appear to be essential for normal proton translocation (12–14). Steady-state measurements of proton pumping in reconstituted vesicles indicate that replacement of aspartic residues at positions 85, 96, or 212 by asparagine partially or completely abolishes proton transport. Partial activities were observed for mutants Asp-115 → Asn or Glu and Tyr-185 → Phe. Replacement of each of the remaining five aspartate residues in bR by asparagine did not have any significant effect on proton transport. Similarly, replacement of each of the other 10 tyrosine residues by phenylalanine had no large effect on steady-state proton pumping. Vibrational spectroscopic studies of the mutants (15, 16) indicate that protonation changes occur in Tyr-185 and Asp-85, -96, and -212 at or before formation of the photointermediate M.

Previously, transient light-induced changes in the electrical conductivity of bR suspensions have been used to detect ion movements with millisecond time resolution (17, 18). This method allows separation in time of the signals due to proton release into, and uptake from, the external aqueous medium after a single turnover flash and also gives the absolute proton quantum yield. The goal of the present experiments has been to measure directly the kinetics and quantum yield of proton release and uptake for the above-mentioned aspartic acid mutants of bR. Our results show that all aspartic acid mutants known to be partially or totally defective in steady-state proton translocation exhibit significant changes in the kinetics and/or yield of proton release and uptake as compared with the wild-type protein. In particular, replacement of Asp-96 by asparagine or Asp-212 by glutamate had marked effects on the kinetics of H^+ uptake. Lower H^+ quantum yields were observed for mutants with asparagine substitutions for Asp-85, -115, and -212.

EXPERIMENTAL METHODS

Preparation of Mutant bR Samples. The construction and cloning of mutant bacterioopsin genes, their expression, and purification in *Escherichia coli* have been described (13, 14, 19–21). The bR-like chromophore was regenerated by the quantitative addition of all-*trans*-retinal to a suspension of the protein in 1% dimyristoyl L-α-phosphatidylcholine/1% CHAPS/0.2% sodium dodecyl sulfate/1.0 or 0.6 mM sodium phosphate buffer, pH 6.0, at 20°C; CHAPS is 3-[(3-cholamidopropyl)dimethylammonio]-1-propanesulfonate. This micellar suspension was used in all of the experiments reported here. Control samples were prepared by deleting retinal or both retinal and the protein in the regeneration mixture.

Conductivity Measurements. The 100-kHz differential ac conductivity apparatus has been described in detail (17, 18). Light excitation brings about conductivity changes by (*i*) the transient release or uptake of small ions (e.g., protons) and (*ii*) the dissipation of the absorbed light into heat, causing a small increase in temperature. The latter increases the conductivity because of the large temperature coefficient of ionic mobility, typically 0.022/°C. This heating produces a

The publication costs of this article were defrayed in part by page charge payment. This article must therefore be hereby marked "*advertisement*" in accordance with 18 U.S.C. §1734 solely to indicate this fact.

Abbreviations: bR, bacteriorhodopsin; ebR, bacteriorhodopsin prepared from the wild-type gene product expressed in *Escherichia coli*. Mutants are indicated by the particular residue that is replaced, with an arrow pointing to the replacement (e.g., Asp-85 → Glu means the aspartic acid residue at position 85 has been replaced by glutamic acid).

shift of the baseline, which is a measure of the number of photons absorbed. The sign and magnitude of the proton conductivity transients depend on the buffer composition: some buffer species such as phosphate anions lose net charge upon protonation, whereas others such as imidazole gain charge. Within our 1-ms time resolution, all such buffer protonation reactions are completed, and proton release or uptake is detected as a change in the relative populations of the acid and base forms of the buffer species. Therefore, the contribution of protons to the signals can be determined by a systematic variation of the buffer composition.

RESULTS

Below, we present the experimental results for wild-type bR expressed in *E. coli* (ebR) and for the mutants with replacements of Asp-85, -96, -115, or -212. In every case, the transients were recorded on two or three time bases to accurately determine the fast and slow components of the changes in conductivity. Time constants ($1/e$) and amplitudes were obtained by nonlinear least-squares fits to the data by using exponential functions of the form $A \exp(-t/\tau)$.

Wild-Type ebR. The effect of varying buffer composition on the conductivity signals for wild-type ebR at pH 6 is shown in Fig. 1. When phosphate was the only buffer species (top trace in Fig. 1), an instantaneous decrease in conductivity was observed, which was followed by an exponential increase over 30 ms. Most of the light energy appeared as heat well within the 1-ms instrumental time resolution, since even by the K intermediate, 70% of the energy of the absorbed photon is converted into heat (22). The observed negative step at $t = 0$ in the top trace of Fig. 1 indicates that a negative transient due to ion movements algebraically sums with the heat step, which is necessarily positive. In phosphate buffer, this is consistent with rapid proton release into the medium—i.e., $HPO_4^{-2} \rightarrow H_2PO_4^-$. Conversely, the slower transient (20–30 ms) reflects proton uptake from the medium. The subsequent traces of Fig. 1 show that with successive additions of imidazole buffer, both the fast and slow transients changed sign. The time constant of the slow phase remained unchanged, indicating that the buffer additions did not perturb the photocycle. The order of proton release and uptake observed here is the same as previously reported for the native purple membrane and for monomeric suspensions of bR in vesicles (18, 23, 24). The technique used here directly measures charge transfer on and off the protein surface, whereas proton transfers inside the protein itself are not observed. Hence, the changes in release and uptake kinetics seen in a given mutant will not necessarily reflect changes in internal H^+ transfers (e.g., protonation/deprotonation of the Schiff base) unless the internal steps are rate-limiting for external charge transfer.

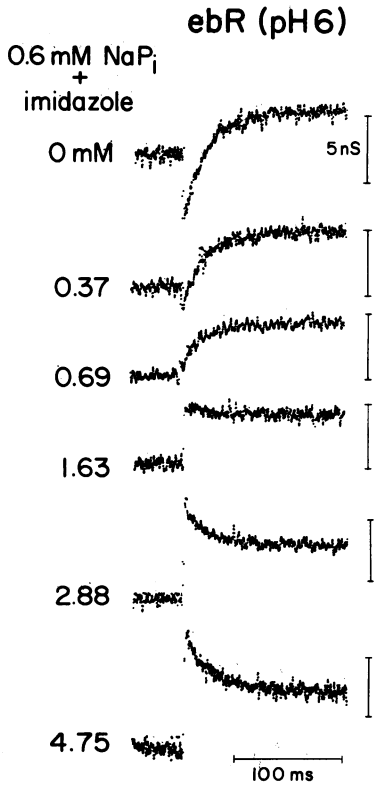

FIG. 1. Regenerated wild-type ebR, pH 6. Buffer titration was started in 0.6 mM sodium phosphate, and imidazole was added at concentrations indicated to the left of each trace. The pHs of the samples are as follows (top to bottom): 6.1, 6.08, 6.05, 6.06, 6.06, and 6.04. Each trace is the sum of 64 sweeps (1000 points, 0.2 ms per point). The vertical bar in each trace is 5 nS (5×10^{-9} ohm^{-1}), and the horizontal bar is 100 ms.

Quantitative analysis of the data was carried out by plotting the observed transient amplitude vs. the calculated conductivity change per equivalent of protons added to each of the buffer mixtures (18, 23, 24). For the data of Fig. 1, the nonproton contribution was small compared with the proton component, and the proton yield was calculated to be 0.063 H^+ per photon absorbed. Table 1 gives a summary of the yields and kinetics for the wild type and the mutants. Experiments with ebR at pH 6.0 and 7.0 gave essentially similar results for the kinetics and quantum yield of proton movement. The quantum yield measured here is also similar to that observed in vesicles (23).

Asp-96 → Asn and Asp-96 → Glu. The light-induced conductivity signals measured for Asp-96 → Asn on both the 200-ms and 10-s time scale at pH 6 are shown in Fig. 2*A*. (In this and subsequent figures, we show only the first and last traces of buffer titrations carried out as in Fig. 1.) In phosphate buffer (upper traces in Fig. 2), a rapid negative step was observed at $t = 0$, similar to that seen in the wild type. However, the time-resolved increase was slowed down

Table 1. Quantum yield and kinetics of proton release and uptake of bR mutants and comparison to steady-state pumping

bR*	pH	ø†	H^+ kinetics,‡ ms		Rel. yield§	Rel. pump¶
			Release	Uptake		
wt	6	0.063	<1	20–25	(1)	(1)
wt	7	0.067	<1	20–30		
D85N	6	0.003‖	—	8–10	0.05	0
D85N	7	0.02‖	—	10–20		
D85E	6	0.023	<1	30–60	0.36	0.32
D85E	7	0.054	<1	100–300		
D96N	6	0.078	<1	500–1000	1.23	0.03
D96N	7	0.057	<1	400–900		
D96E	6	0.061	<1	70–100	0.96	0.83
D96E	7	0.058	<1	100–250		
D115N	6	0.035	70–120	10–20	0.55	0.56
D115E	6	0.018	<1	10–30	0.28	0.32
D115E	7	0.030	<1	10–20		
D212N	6	0.014‖	<1	20	0.22	0.15
D212E	6	0.036	<1	150–250	0.57	0.06

*wt, Wild type; D, Asp; E, Glu; N, Asn.
†Absolute quantum yield of protons per photon absorbed, corrected for light saturation (see ref. 25).
‡Time constants ($1/e$) in ms. Values are upper and lower limits of the range observed for each titration.
§Relative (rel.) yield is the ratio of quantum yield of mutant to that of wild type.
¶Relative (rel.) pump is the ratio of the initial rates of proton pumping of mutant to that of wild type (14), measured at pH 7.
‖Estimated upper bound.

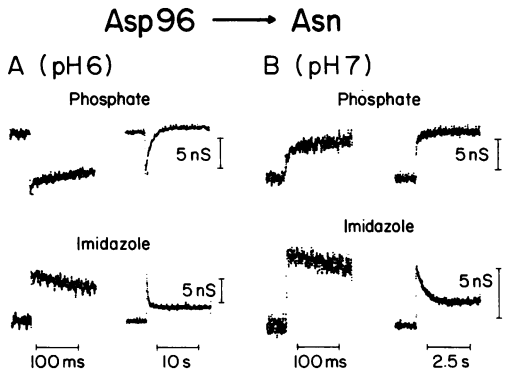

FIG. 2. Asp-96 → Asn mutant at pH 6 (*A*) and pH 7 (*B*). Each set shows the end points of a buffer titration of phosphate with imidazole or vice versa, recorded at two time bases. The buffer in excess in each sample is indicated by the appropriate label. The phosphate and imidazole concentrations (mM) and the pH of each sample, respectively, were: 1, 0, and 6.09 (*A Upper*); 0.97, 4.88, and 6.05 (*A Lower*); 24.6, 4.7, and 6.96 (*B Upper*); and 1, 4.9, and 6.98 (*B Lower*). Each trace is the sum of 16 or 32 flashes.

by well over 1 order of magnitude. The addition of excess imidazole (lower traces in Fig. 2) clearly reversed the sign of both the fast step and the resolved decay, indicating that the bulk of the ion movements are due to protons. These data show that, after illumination, protons are rapidly released into the aqueous phase and then taken up on the time scale of 0.5–1 s. Similar results were obtained at pH 7 (Fig. 2*B*), except that the quantum yield was slightly lower (Table 1), as was the uptake time constant (0.4–0.9 s). In both cases, however, proton release occurred within 1 ms, and the proton quantum yield was essentially similar to that of ebR. In contrast, the signals for the Asp-96 → Glu mutant (Fig. 3) were closer to those of the wild type, although the uptake time constant was longer: 70–100 ms at pH 6 and 100–250 ms at pH 7. The quantum yield and proton release kinetics were also similar to those of ebR (Table 1).

Asp-85 → Asn and Asp-85 → Glu. For the Asp-85 → Asn mutant at pH 6, a rapid unresolved increase in conductivity was observed at $t = 0$ (Fig. 4*A*, upper traces). This was followed by an increase on the 10-ms time scale and an apparent slow decrease over several seconds. Addition of excess imidazole buffer (Fig. 4*A*, lower traces) caused no qualitative change in the transients. The difference between the upper and lower traces in Fig. 4*A* corresponds to a small proton uptake signal, comparable to the noise, with a 10-ms time constant. The H^+ quantum yield estimated from this

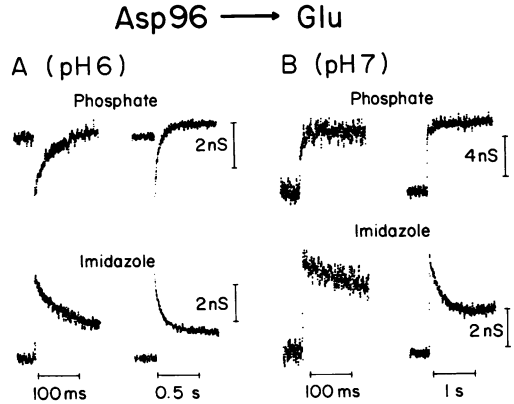

FIG. 3. Asp-96 → Glu mutant at pH 6 (*A*) and pH 7 (*B*). The presentation is as in Fig. 2. The phosphate and imidazole concentrations (mM) and the pH of each sample, respectively, were: 1, 0, and 6.1 (*A Upper*); 1, 9.2, and 6.03 (*A Lower*); 39.6, 8.2, and 6.97 (*B Upper*); and 0.92, 8.6, and 7.07 (*B Lower*). All traces are the sum of 64 flashes.

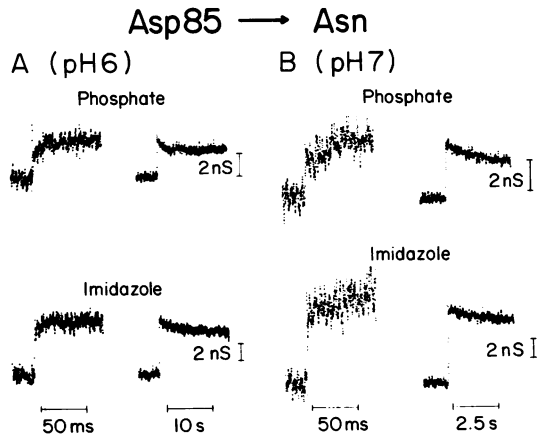

FIG. 4. Asp-85 → Asn mutant at pH 6 (*A*) and pH 7 (*B*). The buffer titration was as in Fig. 2. The phosphate and imidazole concentrations (mM) and the pH of each sample, respectively, were: 1, 0, and 5.95 (*A Upper*); 0.97, 10.9, and 6.04 (*A Lower*); 1, 0, and 7.03 (*B Upper*); and 1, 8.1, and 7.02 (*B Lower*). All traces are the sum of 64 flashes.

experiment is 0.003, which is about 1/20th that observed for ebR. The quantum yield as well as the signal difference caused by the buffer change were larger at pH 7 (Fig. 4*B*). Because of the small size of the difference transient, it cannot be excluded that proton release is rapid and that the slow conductivity changes are caused by extraneous relaxations of similar size and magnitude (see *Discussion*). In this case, the estimated quantum yields for this mutant in Table 1 are upper bounds.

Fig. 5 shows the results for the Asp-85 → Glu mutant at pH 6 and 7. These signals closely match the transients seen for ebR. The proton release step occurred within 1 ms at both pH values, but the uptake step at pH 7 (≈200 ms) was slower than that at pH 6 (≈50 ms).

Asp-115 → Asn and Asp-115 → Glu. The conductivity signals for the Asp-115 → Asn mutant represent an example where the release of heat and the release and uptake of protons were each resolved clearly (Fig. 6*A*). Two distinct kinetic phases were observed on the 100-ms time scale after the positive step at $t = 0$ due to heating, and both kinetic phases clearly reversed sign when the phosphate buffer was titrated with imidazole. Within experimental error, only protons contribute to both the phases, and the concentrations of protons taken up and released were equal. The proton uptake step had a time constant of 10–20 ms, comparable to

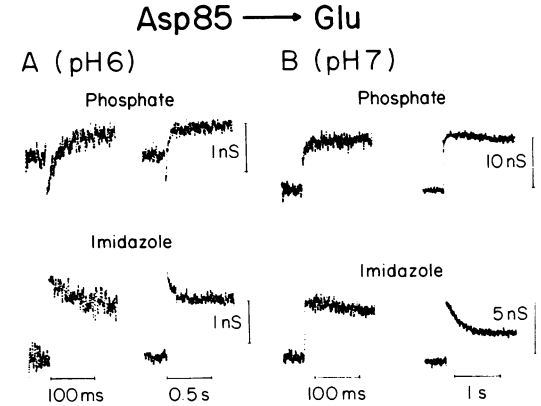

FIG. 5. Asp-85 → Glu mutant at pH 6 (*A*) and pH 7 (*B*). The buffer titration was as in Fig. 2. The phosphate and imidazole concentrations (mM) and the pH of each sample, respectively, were: 1, 0, and 6.00 (*A Upper*); 1, 6, and 6.03 (*A Lower*); 42.1, 5.63, and 6.98 (*B Upper*); and 1, 5.94, and 7.01 (*B Lower*). All traces are the sum of 64 flashes.

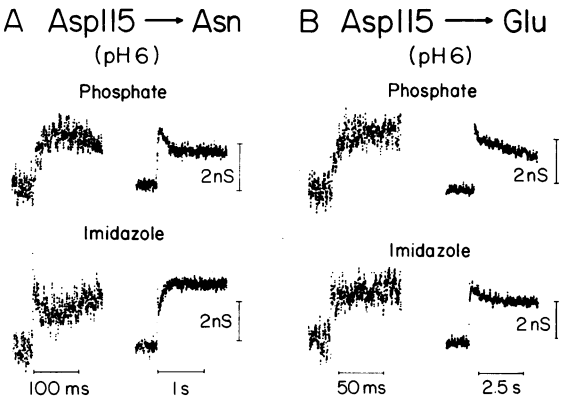

FIG. 6. Asp-115 mutants at pH 6. Replacement by asparagine (*A*) and glutamic acid (*B*). The phosphate and imidazole concentrations (mM) and the pH of each sample, respectively, are: 1, 0, and 5.98 (*A Upper*); 0.97, 9.1, and 5.98 (*A Lower*); 1, 0, and 5.99 (*B Upper*); and 1, 9.2, and 6.00 (*B Lower*). All traces are the sum of 64 transients.

that of wild type, but the release step was slowed down to about 100 ms. The quantum yield obtained from these measurements was 0.035 protons per photon absorbed, which is about half of the wild-type yield.

The results for the glutamate substitution of Asp-115 (Fig. 6*B*) indicate that nonproton ion movements contributed significantly to the observed conductivity signals because addition of excess imidazole did not completely invert the sign of the transient. However, the kinetics of the proton release and uptake components of the signal were indistinguishable from those for wild type. The quantum yields at pH 6 and pH 7 were 0.018 and 0.03, respectively.

Asp-212 → Asn and Asp-212 → Glu. At pH 6.0, conductivity signals observed for the Asp-212 → Glu mutant (Fig. 7) correspond to rapid proton release followed by slow uptake (150–250 ms), with a quantum yield of 0.036 (56% of wild type). The traces of Fig. 7 show a reversal of sign upon buffer titration, indicating that for this mutant, protons are the major mobile ionic species following light excitation. This mutant has a broadened absorption spectrum with a maximum at 580 nm, and the reduction in quantum yield may reflect the presence of a less active blue form of the chromophore. Experiments on the Asp-212 → Asn mutant were complicated by the light-induced destabilization of the chromophore and the necessity of using repetitive flashes. The conductivity signals showed a large contribution from the transient movements of nonproton ions. The kinetics of the low-amplitude H^+ component was measured independently by forward and reverse titration and was found to be similar to that of ebR.

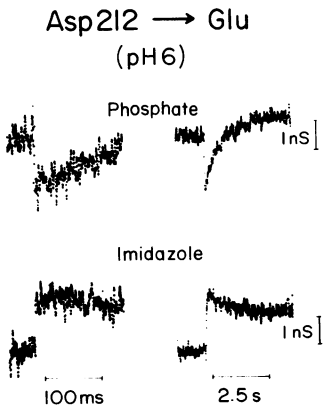

FIG. 7. Asp-212 → Glu mutant at pH 6. The buffer titration was as in Fig. 2. The phosphate and imidazole concentrations (mM) and the pH of each sample, respectively, are 1, 0, and 5.99 (*Upper*) and 0.98, 6.15, and 6.04 (*Lower*). All traces are the sum of 64 transients.

DISCUSSION

The experiments presented here provide significant insights into the recently reported effects of aspartic acid replacements on steady-state proton transport in bR (14). Time-resolved conductivity measurements allow separation of the kinetic and yield defects in the mutants. All mutants defective in proton pumping showed differences in the yield and/or kinetics of H^+ release and uptake.

Both the Asp-96 → Asn and the Asp-96 → Glu mutants form chromophores with absorption maxima close to that of ebR. However, the Asp-96 → Asn mutant showed a reduction to 1/25th in the rate of proton uptake without any effect on the rate of proton release. A much smaller effect on the uptake kinetics was observed for the corresponding glutamate substitution (Table 1), and the observed quantum yields of both mutants were similar to that of ebR. Therefore, we conclude that the carboxylic group of Asp-96 plays a critical role in reprotonation but has little effect on either the kinetics or the efficiency of proton release during the photocycle. That is, in the normal operation of the pump, the events leading to proton release occur regardless of the presence or absence of a carboxyl group at position 96.

The Asp-85 → Asn mutation causes a dramatic decrease in the quantum yield, especially at pH 6. The proton-uptake kinetics closely match those of ebR. However, it is difficult to make a clear statement about the kinetics of proton release, partly because of the low signal-to-noise ratios (Fig. 4). It is possible that the 1- to 2-s transient reflects a slow proton-release step. This would be consistent with the observation that the conductivity baseline at long times is close to that extrapolated to $t = 0$—i.e., most of the instantaneous (<1 ms) conductivity change is due to heat alone and not due to fast ion movements. Alternatively, the transient could be caused by light-induced volume fluctuations or by thermal drifts. Such slow relaxations on the time scale of several seconds are observed even in control samples that lack retinal.

Wild-type proton-uptake kinetics are observed with the Asp-212 → Asn mutant, but with lower quantum yields. Optical spectroscopic work also indicates that the yield for the formation of an M-like intermediate is low for this mutant (L. Stern, T. Mogi, T. Marti, H.G.K., and K. J. Rothschild, unpublished data). In contrast to the Asp-85 and -96 mutants, the proton-uptake kinetics of the Asp-212 → Glu mutant are slower than those for the corresponding asparagine mutant. Higher activities are also found for the Asp-212 → Asn mutant in steady-state pumping experiments (14). These observations suggest structural and/or regulatory functions for Asp-212, apart from its role as a proton donor and acceptor.

The absorption maxima of the Asp-85 and -212 mutants are markedly red-shifted. In particular, the Asp-85 → Glu mutant exhibits a blue-to-purple transition between pH 6 and pH 7. Hence, interpretation of the changes in the yield of proton pumping and kinetics is ambiguous because there may be a mixture of the two forms of the chromophore. The observed decreases in yield may not be due to the simple loss of a proton-carrying COOH group in an otherwise normal bR molecule. In this regard, the Asp-85 → Glu mutant, which is predominantly in the purple form at pH 7, shows a quantum yield closer to wild type than at pH 6, when it is blue.

As determined by the conductivity transients, proton release for the Asp-115 → Asn mutant is much slower than for ebR and, in fact, is slower than proton uptake. This apparent reversal in the normal temporal order of release and uptake provides a highly significant clue to the mechanism of proton translocation. Just as the Asp-96 → Asn mutation shows an alteration only in the uptake kinetics, the Asp-115 → Asn mutation affects only the kinetics of proton release. Taken

together, these results imply that the release and uptake steps of the pump are functionally decoupled. This would argue that the primary photochemistry of bR sets in motion events leading separately to proton release and uptake—i.e., H^+ release into the aqueous medium is not a prerequisite for H^+ uptake from the medium, or vice versa.

The mutants examined here were chosen because of their effects on steady-state proton translocation in reconstituted vesicles (14). The pumping rates observed in steady-state experiments are determined by both the lifetime of the photocycle—i.e., the turnover time of the pump—and by its quantum yield. Therefore, reduced rates can be caused both by an increased lifetime or by a lower quantum yield. Our results show that the low pumping observed for the Asp-96 → Asn mutant is due to a slow reprotonation and not to a change in the quantum yield. The idea that Asp-96 → Asn is kinetically incompetent fits well with recent optical and photoelectric measurements on this mutant (M. P. Heyn, M. Holz, H. Otto, T. Mogi, and H.G.K., unpublished data). In contrast, the partial activities observed for the Asp-115 mutants are due, at least in part, to reductions in the quantum yield. Similarly, a low quantum yield could be the main reason for lack of proton pumping activity in the Asp-85 → Asn mutant. With the exception of Asp-212, replacements of aspartate by glutamate always resulted in smaller changes in the kinetics and quantum yield than for the corresponding replacements by asparagine. In Table 1 wherever there is a major discrepancy between the relative quantum yields and relative pumping activities, the mutant (Asp-96 → Asn and Asp-212 → Glu) shows a significant increase in the cycle time of the pump.

A large number of bR mutants containing amino acid replacements are now available for structure–function studies. These mutants have been investigated by a combination of spectroscopic (15, 16, 26) and electrochemical methods. Time-resolved conductivity measurements directly probe proton transfers between the protein and the aqueous phase. In particular, the present experiments show that specific aspartic residues participate in separate stages of the photocycle and represent a step toward further clarification of the molecular mechanism of proton transport.

This work was supported by grants from the National Institutes of Health (R01 GM28289-07); the Office of Naval Research, Department of the Navy (N00014-82-K-0668); and the National Science Foundation (NSF PCM-81-10992) to H.G.K. and by National Institutes of Health Grant GM32955-03/04 to T. Marinetti. S.S. is supported by a Damon Runyon–Walter Winchell Cancer Fund Fellowship (DRG-937), and T. Marti is the recipient of a fellowship from the Swiss National Science Foundation.

1. Oesterhelt, D. & Stoeckenius, W. (1973) *Proc. Natl. Acad. Sci. USA* **70,** 2853–2857.
2. Stoeckenius, W. & Bogomolni, R. A. (1982) *Annu. Rev. Biochem.* **52,** 587–616.
3. Hsieh, Ch.-L., Nagumo, M., Nicol, M. & El-Sayed, M. A. (1981) *J. Phys. Chem.* **85,** 2714–2717.
4. Braiman, M. & Mathies, R. (1982) *Proc. Natl. Acad. Sci. USA* **79,** 403–407.
5. Lozier, R. H., Niederberger, W., Bogomolni, R. A., Hwang, S.-B. & Stoeckenius, W. (1976) *Biochim. Biophys. Acta* **440,** 545–556.
6. Lozier, R. H., Bogomolni, R. A. & Stoeckenius, W. (1975) *Biophys. J.* **15,** 955–962.
7. Xie, A. H., Nagle, J. F. & Lozier, R. H. (1987) *Biophys. J.* **51,** 627–635.
8. Rothschild, K. J., Zagaeski, M. & Cantore, W. A. (1981) *Biochem. Biophys. Res. Commun.* **103,** 483–489.
9. Engelhard, M., Gerwert, K., Hess, B. & Siebert, F. (1985) *Biochemistry* **24,** 400–407.
10. Eisenstein, L., Lin, S.-L., Dollinger, G., Odashima, K., Termini, J., Konno, K., Ding, W.-D. & Nakanishi, K. (1987) *J. Am. Chem. Soc.* **109,** 6860–6862.
11. Khorana, H. G. (1988) *J. Biol. Chem.* **263,** 7439–7442.
12. Hackett, N. R., Stern, L. J., Chao, B. H., Kronis, K. A. & Khorana, H. G. (1987) *J. Biol. Chem.* **262,** 9277–9284.
13. Mogi, T., Stern, L. J., Hackett, N. R. & Khorana, H. G. (1987) *Proc. Natl. Acad. Sci. USA* **84,** 5595–5599.
14. Mogi, T., Stern, L. J., Marti, T., Chao, B. H. & Khorana, H. G. (1988) *Proc. Natl. Acad. Sci. USA* **85,** 4148–4152.
15. Braiman, M. S., Mogi, T., Stern, L. J., Hackett, N. R., Chao, B. H., Khorana, H. G. & Rothschild, K. J. (1988) *Proteins: Struct. Funct. Genet.* **3,** 219–229.
16. Braiman, M. S., Mogi, T., Marti, T., Stern, L. J., Khorana, H. G. & Rothschild, K. J. (1988) *Biochemistry* **27,** 8516–8520.
17. Marinetti, T. & Mauzerall, D. (1983) *Proc. Natl. Acad. Sci. USA* **80,** 178–180.
18. Marinetti, T. & Mauzerall, D. (1986) *Biophys. J.* **50,** 400–415.
19. Nassal, M., Mogi, T., Karnik, S. S. & Khorana, H. G. (1987) *J. Biol. Chem.* **262,** 9264–9270.
20. Karnik, S. S., Nassal, M., Doi, T., Jay, E., Sgaramella, V. & Khorana, H. G. (1987) *J. Biol. Chem.* **262,** 9255–9263.
21. Braiman, M. S., Stern, L. J., Chao, B. H. & Khorana, H. G. (1987) *J. Biol. Chem.* **262,** 9271–9276.
22. Birge, R. R. & Cooper, T. M. (1983) *Biophys. J.* **42,** 61–69.
23. Marinetti, T. (1987) *Biophys. J.* **52,** 115–121.
24. Marinetti, T. (1987) *Biophys. J.* **51,** 875–881.
25. Marinetti, T. (1988) *Biophys. J.* **54,** 197–204.
26. Ahl, P. L., Stern, L. J., During, D., Mogi, T., Khorana, H. G. & Rothschild, K. J. (1988) *J. Biol. Chem.* **263,** 13594–13601.